


## Article

# Facile Preparation of Biocompatible and Transparent Silica Aerogels as Ionogels Using Choline Dihydrogen Phosphate Ionic Liquid

Seeni Meera Kamal Mohamed<sup>1,2</sup>, Rajavelu Murali Sankar<sup>1</sup>, Manikantan Syamala Kiran<sup>3</sup>,  
Sellamuthu N. Jaisankar<sup>1</sup>, Barbara Milow<sup>2,\*</sup>  and Asit Baran Mandal<sup>1,4,5,\*</sup>

- <sup>1</sup> Polymer Science & Technology Division, Council of Scientific & Industrial Research (CSIR)-Central Leather Research Institute (CLRI), Adyar, Chennai 600020, Tamil Nadu, India; seenimeera.kamal Mohamed@dlr.de (S.M.K.M.); muralicri@gmail.com (R.M.S.); snjai@hotmail.com (S.N.J.)
- <sup>2</sup> Department of Aerogels and Aerogel Composites, Institute of Materials Research, German Aerospace Center (DLR), Linder Hoehe, 51147 Cologne, Germany
- <sup>3</sup> Biological Materials Laboratory, Council of Scientific & Industrial Research (CSIR)-Central Leather Research Institute (CLRI), Adyar, Chennai 600020, Tamil Nadu, India; kiran@clri.res.in
- <sup>4</sup> Inorganic & Physical Chemistry Laboratory, Council of Scientific & Industrial Research (CSIR)-Central Leather Research Institute (CLRI), Adyar, Chennai 600020, Tamil Nadu, India
- <sup>5</sup> Council of Scientific & Industrial Research (CSIR)-Central Glass and Ceramic Research Institute (CGCRI), 196 Raja S.C. Mullick Road, Jadavpur, Kolkata 700032, India
- \* Correspondence: barbara.milow@dlr.de (B.M.); abmandal@cgcri.res.in (A.B.M.);  
Tel.: +49-2203-601-3537 (B.M.); +91-33-2322-3402 or +91-33-2473-5829 or +91-33-2483-9241 (A.B.M.);  
Fax: +91-33-2473-0957 or +91-33-2483-9241 (A.B.M.)

**Featured Application:** Ionogels containing bio-ionic liquids help in the area of biomolecule encapsulation. Bio-ionic liquids can retain the stability of biomolecules at room temperature within the pores of ionogels. Ionogels have interesting applications in biosensors, electrochemical devices, super capacitors, batteries, gas sensors, CO<sub>2</sub> capture, and so forth.



**Citation:** Kamal Mohamed, S.M.; Murali Sankar, R.; Kiran, M.S.; Jaisankar, S.N.; Milow, B.; Mandal, A.B. Facile Preparation of Biocompatible and Transparent Silica Aerogels as Ionogels Using Choline Dihydrogen Phosphate Ionic Liquid. *Appl. Sci.* **2021**, *11*, 206. <https://doi.org/10.3390/app11010206>

Received: 3 December 2020

Accepted: 23 December 2020

Published: 28 December 2020

**Publisher's Note:** MDPI stays neutral with regard to jurisdictional claims in published maps and institutional affiliations.



**Copyright:** © 2020 by the authors. Licensee MDPI, Basel, Switzerland. This article is an open access article distributed under the terms and conditions of the Creative Commons Attribution (CC BY) license (<https://creativecommons.org/licenses/by/4.0/>).

**Abstract:** We developed a facile and greener approach for the preparation of silica-aerogel-based ionogels using choline dihydrogen phosphate ionic liquid by the sol-gel approach. A series of silica-based aerogels as ionogels were prepared by varying the ionic liquid concentrations: 0.1, 0.5, 1, 3, 5, and 10 wt %. The as-prepared ionogels were characterized using several analytical techniques, namely, attenuated total reflectance (ATR)/FT-IR, TGA, XRD, and particle size analyses. The role of ionic liquid in the viscoelastic properties of the sol-gel transition was monitored using time-dependent rheological measurements. The addition of ionic liquid to the sol-gel system favored the formation of a more interconnected silica network structure. The formation of a silica network structure during sol-gel hydrolysis and condensation was confirmed from <sup>29</sup>Si solid-state CP/MAS NMR spectra. The effect of the ionic liquid on the morphological properties was investigated using SEM and TEM studies. The cell viabilities of the prepared gel samples were clearly evident from the cytotoxicity assay studies using Swiss and HaCaT cells. The main advantages of using biocompatible ionic liquids for the preparation of these aerogels as ionogels are that they may be used for encapsulating biological molecules and retain their conformational stability for a longer duration.

**Keywords:** aerogels; ionogels; silica; ionic liquid; choline dihydrogen phosphate

## 1. Introduction

Silica aerogels have received much attention recently owing to their exceptional properties such as low density (0.003–0.8 g/cm<sup>3</sup>), large porosity (>90% having pore sizes ranging from 5 to 100 nm), high surface area, low thermal conductivity, and so forth [1–3]. These superior properties of aerogels make them useful for applications in the fields of

optical sensors, biomolecule encapsulation, catalysis, adsorbents, chemical separation, drug delivery, and aerospace [4–6]. However, the traditional synthesis of silica aerogels involves the hydrolysis and condensation of tetraalkoxysilane precursors using a mildly acidic or basic catalyst followed by a drying process. The release of alcohol (from silane precursors) has detrimental effects on the activity of biomolecules during hydrolysis [7]. Moreover, the conventional drying process can cause up to 80% shrinkage of the gel network, resulting in limited entrapment of biomolecules. This limits the application of silica aerogel in the fields of biomolecule encapsulation and biosensors due to slow response time [8]. The encapsulation of biomolecules inside the gel matrix can be achieved *in situ* or after supercritical drying to eliminate network collapse. However, harsh supercritical drying can easily damage the biomolecule structure [9,10]. To avoid this problem, ionic liquids (ILs) were recently used as green solvents for the preparation of sol–gel-derived silica-based aerogels [11–13]. Ionic liquids can control the structure of silica (i.e., pore size, structure, and distribution) apart from the type of catalyst, water content, solvent, and template used [14–16]. In addition, ILs can avoid the problem of gel shrinkage and act as a pore-forming template during the sol–gel formation. Ionic liquids can be confined inside the pores of silica aerogel, which act as a protective agent for the encapsulated biomolecules, thereby retaining their conformational stability [17]. The use of different ionic liquids for the preparation of silica aerogel was attempted by several researchers over the years [18–20]. Dai et al. [18] reported the preparation of silica aerogel using imidazolium-based ionic liquids, which eliminated the risky supercritical drying process. ILs based on the salts of imidazolium ions were used as a morphology controller and precatalyst for the preparation of silica xerogel [19]. Additionally, ILs could be used as a drying control chemical additive during the sol–gel transition, which prevents the strain associated with the evaporation of solvents [20].

Ionogels are a new class of materials that emerged recently that are prepared using ionic liquids in which the ionic liquid is confined inside the nanopores of the silica gel matrix [21–23]. These solid-like macroscopic materials exhibit superior properties, which do not flow at room temperature compared with bulk ionic liquids [21,24–26]. The properties include luminescence, transport, and high ionic or electronic conductivity [27,28]. Novel ionogels were prepared using tamarind gum and ILs (1-butyl-3-methylimidazolium chloride and 1-butyl-3-methylimidazolium bromide), which have shown good adherence to human finger muscles and skin. These novel ionogels may find applications in electrochemical biosensors, actuators, and biomaterials [29]. Ionogels prepared by utilizing 1-methyl-3-butylimidazolium ibuprofenate with a minimal amount of solvent can be used as an efficient drug delivery system and the drug release kinetics can be controlled by the nature of the silica wall surface [30]. Furthermore, 1-butyl-3-methylimidazolium tetrafluoroborate IL was used to make a gel of low-molecular-weight iron dextran complex, which has applications in medical electrosensitive gel device fabrications [31]. Very recently, new types of nanocomposites containing agarose-chitosan-1-butyl-3-methylimidazolium chloride solutions were developed using an antisolvent method, suitable for sensors, solar cells, and electronic device materials [32]. In the recent times, ionic-liquid-anchored silica particles have been used in making polymer nanocomposites with enhanced properties, especially mechanical, thermal, and proton conductivity, for polymer electrolyte membrane fuel cell applications [33–35]. Moreover, immobilizing ionic liquids on xerogel silica helped researchers to achieve a solid–gas system for CO<sub>2</sub> capture [36].

In most cases, imidazolium-based ionic liquids were used as templates and structure-directing agents for the preparation of sol–gel-derived silica aerogels and ionogels [12]. However, Lee et al. [37] used an ionic liquid as an additive to prevent the inactivation of enzymes during the sol–gel process, which retains 80% of the enzyme activity compared with enzymes encapsulated in gel without an ionic liquid. The enhanced activity and thermal stability of the horseradish peroxidase enzyme were achieved by encapsulating it in a room temperature ionic-liquid-based sol–gel matrix [38]. In the recent past, Li et al. [9] demonstrated the preparation of a red fluorescent protein encapsulated bio-aerogel using

1-butyl-3-methylimidazolium chloride ionic liquid as a solvent and pore-forming agent. Here, 85% fluorescent activity of the protein was retained. Most of the ILs comprising imidazolium cations have been found to exhibit toxicity, sometimes more toxic than conventional organic solvents [39]. ILs containing imidazolium, pyridinium cations, and halide anions have been found to be highly toxic and less biodegradable, which can create aquatic environmental problems due to leaching into water resources [40].

Recently, researchers have focused on the use of ionic liquids prepared from cations and anions of biological components with well-studied biological and biodegradation properties [34,35,41,42], in particular, a choline-cation-based ionic liquid, which is an important cation present in the liver that regulates biological metabolism in the human body [41–44]. There are several ionic liquids reported to have different anions such as formate, lactate, dihydrogen phosphate, levulinate, and so forth, in combination with choline cations. Naturally, choline and phosphate ions are present in the human body, so the combination of these cations and anions is of interest. Choline dihydrogen phosphate (CDHP) is an important bio-ionic liquid reported to have the combination of chaotropic cations and kosmotropic anions, which can stabilize proteins in aqueous solutions [45]. Moreover, Fujita et al. [46] also reported a series of choline-based ionic liquids that can dissolve proteins and retain their secondary structure at high temperatures. The structural stability and activity of cytochrome *c* in the hydrated form of choline dihydrogen phosphate IL was clearly demonstrated by Weaver et al. [47] using different techniques. According to Fujita et al. [48], cytochrome *c* retains its native state and remains active for 18 months during storage at room temperature in hydrated choline dihydrogen phosphate IL compared to ILs from various anions such as dibutyl phosphate, acetate, lactate, and methane sulfonate. The high solubility of DNA from salmon testes was achieved by dissolving it in choline-based ionic liquids, and the recyclability of IL was found to be very good (95%) [49]. Specifically, CDHP is an important candidate for the encapsulation of biomolecules into a silica gel matrix [50]. The hydrated form of CDHP ionic liquid greatly improved the thermodynamic stability of DNA duplex, which opens up a new pathway for the development of biomaterials from DNA base pair switches [51]. Recently, we reported for the first time the use of a choline formate IL for preparing biocompatible and surface-active silica aerogels with 90% cell viability and proliferation compared with control gel without IL [52,53]. In this study, our main approach was to prepare silica-based ionogels using biocompatible CDHP ionic liquid as a green solvent and to study the role of ionic liquid concentration on its properties.

In the current work, we developed a facile and greener approach for the preparation of silica aerogels as ionogels using choline dihydrogen phosphate ionic liquid as a green solvent. The prepared ionogels were characterized using several physicochemical analytical techniques, namely, attenuated total reflectance (ATR)/FT-IR, TGA, particle size analysis, XRD, small-angle X-ray scattering (SAXS), SEM, and TEM, to study the effect of IL on the properties of ionogels. The viscoelastic properties of the prepared silica sol solution were also monitored using time-dependent rheological measurements.

## 2. Materials and Methods

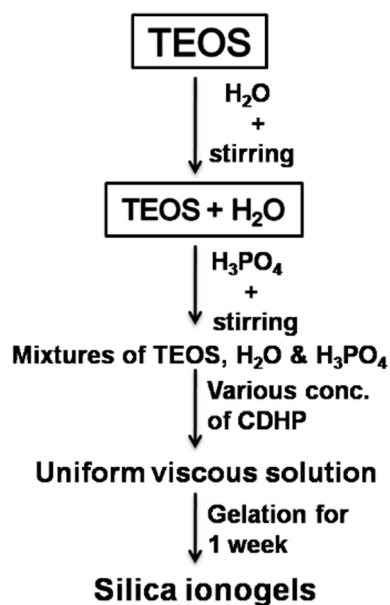
### 2.1. Materials

Choline dihydrogen phosphate (98%) was purchased from Carl Roth, Germany. Tetraethylorthosilicate (TEOS), MTT [3-(4,5-dimethylthiazol-2-yl)-2,5-diphenyltetrazolium bromide], *ortho*-phosphoric acid (H<sub>3</sub>PO<sub>4</sub>), and Dimethyl sulfoxide (DMSO) were purchased from Sigma Aldrich, USA. Cell lines (Swiss and HaCaT) were obtained from National Centre for Cell Science, Pune. Millipore water was used throughout the experiments. All the reagents and chemicals were used as received.

### 2.2. Preparation of Silica Ionogels

The synthesis of silica ionogels was performed in an aqueous medium at room temperature (RT). Control silica gel was prepared as follows: 1 mL of TEOS was taken in a sample vial and 2 mL of water was mixed with TEOS precursor under magnetic stirring at RT

(25 °C). Then, 0.5 mL of  $\text{H}_3\text{PO}_4$  was added dropwise into it with stirring and the stirring continued for another 15 min to get a uniform solution. The mixture was covered by parafilm with small holes for the evaporation of solvents. Further, the solution underwent gelation at RT for over a week and was freeze-dried. The simple schematic representation of the ionogel synthesis strategy is given in Scheme 1.



**Scheme 1.** Simple schematic representation of silica ionogel preparation.

The same methodology was adopted to prepare ionogels using choline dihydrogen phosphate IL. To the mixtures of TEOS,  $\text{H}_2\text{O}$ , and  $\text{H}_3\text{PO}_4$ , various concentrations of IL were added to it and stirred for 15 min to get the true solution. They were then covered with parafilm with small holes and further allowed for gelation at RT for 1 week. After 1 week, the gels were taken out and freeze-dried to remove the moisture and solvents. Further, they were ground well to get a powder form for different analyses. The ratio of  $\text{TEOS}:\text{H}_2\text{O}:\text{H}_3\text{PO}_4$  was maintained as 1:2:0.5 throughout the experiments. The IL concentration was varied as 0.1, 0.5, 1.0, 3.0, 5.0, and 10.0 wt. %. Table 1 represents the formulation of sol–gel-based silica ionogels.

**Table 1.** Formulations of the sol–gel-based silica ionogels.

Codes	TEOS:H <sub>2</sub> O:H <sub>3</sub> PO <sub>4</sub>	IL (wt. %)	Gelation Time (min) <sup>a</sup>
IL 0		0	195
IL 0.1		0.1	185
IL 0.5		0.5	170
IL 1.0	1:2:0.5	1.0	165
IL 3.0		3.0	155
IL 5.0		5.0	140
IL 10.0		10.0	120

<sup>a</sup> obtained by monitoring sol–gel transition at room temperature (RT).

### 2.3. Characterization of Ionogels

FT-IR spectra for wet and dried gel samples were collected using an attenuated total reflectance (ATR)/FT-IR spectrometer (ABB MB 3000, Canada) over the range of 4000–600  $\text{cm}^{-1}$  with a scan of 60 scans/s and resolution of 16  $\text{cm}^{-1}$ . The gel samples were placed over a zinc selenide (ZnS) surface. The angle of incidence of the infrared beam onto the surface was 45°. The standard calibration of the instrument was done

by measuring the spectra of polystyrene film over the crystal surface as a calibration standard. Thermogravimetric studies were performed using TG analyzer Model Q50 (TA Instruments) with a heating rate of 20 °C/min under N<sub>2</sub> atmosphere from 30 to 800 °C. The formation of a siloxane network structure in the prepared gel was characterized by using <sup>29</sup>Si solid-state NMR spectra, Bruker Avance 400 spectrometer, Germany, at a frequency of 79.49 MHz for <sup>29</sup>Si cross-polarization magic-angle-spinning (CP/MAS) NMR. The particle size measurements for the ground gel powder were performed using a Yobin Horiba, LB-550, particle size analyzer by making a dilute dispersion of silica particles in deionized water. The sol–gel transition was monitored using rheological experiments in a cone-plate geometry (CP 25-1) using an Anton Paar Physica rheometer (MCR301) with oscillatory tests. The measurements were performed at a constant frequency (1 Hz) and constant strain of 1% at 25 °C with time variation. X-ray diffraction patterns for the prepared gels were analyzed using an X-pert PRO X-ray diffractometer under Cu K $\alpha$  radiation ( $\lambda = 1.54 \text{ \AA}$ ) under a voltage of 40 kV and a current density of 40 mA, scanning over a range of 3°–80° at a rate of 4°/min. Small-angle X-ray scattering (SAXS) measurements of gel samples were performed using a SAXSpace instrument from Anton Paar with the following specifications: collimation: line collimation; time: 30 s  $\times$  40 frames (20 min); analysis: SAXStreat and SAXSQuant software; detector: Mythen 2 (1D detector); temperature: 28 °C; holder: solid sample holder; q range of 0.1–10 nm<sup>-1</sup> under Cu K $\alpha$  radiation ( $\lambda = 0.071 \text{ nm}$ ). The structural morphology of the prepared silica gels was obtained using scanning electron microscopy (JEOL, JEM-7500F, Japan). TEM images were examined using a transmission electron microscope (JEOL, JEM-1200EX, Japan).

### 3. Results

#### 3.1. FT-IR Spectra

FT-IR spectra for the prepared silica ionogels in wet and drying conditions are given in Figure S1. The appearance of a broad peak in the region of 3200–3700 cm<sup>-1</sup> is the characteristic of the O-H stretching vibration of the Si-OH groups present in the gel, and overlapping of H<sub>2</sub>O vibration was observed [54,55]. The peak at 1088 cm<sup>-1</sup> (Figure S1b) is due to the presence of Si-O stretching vibration ( $\nu_{\text{Si-O}}$ ) and another peak at around 800 cm<sup>-1</sup> is the characteristic of O-Si-O stretching vibration. The characteristic peaks of the ionic liquid (CDHP) were observed in the spectra of ionogels at 1080 and 955 cm<sup>-1</sup> (Figure 1), corresponding to P=O and P-OH of dihydrogen phosphate ions, respectively [56]. Further, the appearance of the peak in the range of 2826–2996 cm<sup>-1</sup> (Figure S1a) is mainly due to the alkyl groups of ethanol formed during the sol–gel reaction, which completely disappeared in the spectra of the freeze-dried gel (Figure S1b). The introduction of higher ionic liquid concentrations increased the intensity and broadening of the peak position of Si-O stretching vibration. This clearly indicates that the introduction of an ionic salt (CDHP) promotes the formation of highly dense silica networks, thereby strengthening the silica gel structure. The increase in the intensity of the Si-O vibration of ionogels confirms the presence of strong ionic interaction between silica particles and ionic liquid, which was also proved from the particle size measurements (Figure S4).

#### 3.2. TGA Analyses

The thermal stability of the wet gel was determined using TGA, and their respective thermograms are depicted in Figure S2. All the gel samples exhibited weight loss at around 100 °C, which corresponds to the elimination of alcohol and residual water formed during the sol–gel hydrolysis of alkoxy silane and condensation of silanol groups [57]. The % weight loss at 100 °C is given in Table 2.

The % weight loss at 100 °C for control gel (without IL) was found to be 13.1%, whereas gel prepared with a higher IL content (IL 10.0) shows 8.5%. The confinement of ionic liquid inside the pores of the silica gel matrix prevents the evaporation of solvent formed during hydrolysis and condensation stages. However, higher temperatures (>100 °C) can cause the continuous evaporation of bound water adsorbed on the pore walls of the silica matrix.

The minimum weight loss at 100 °C is similar to that reported by Ashby et al. [58] for silica ionogels. The decrease in weight loss percent at 100 °C provides evidence about the confinement of IL in the pores of gels [59]. The wet silica gel samples exhibiting weight loss at around 150 °C could be attributed to the loss of bound water present in the pores of the gel and some hydroxyl groups present on the surface [19]. Yoshizawa-Fujita et al. [60] reported that dihydrogen phosphate salt is thermally stable up to 200 °C. Here, the gels prepared with IL showed weight loss at onset temperature 200 °C due to the presence of IL in the gel matrix [61]. Further, significant weight loss was observed at around 350 °C, which is attributed to the thermal decomposition of organic moieties present in the gels [62]. Moreover, silica provides more protection to the entrapped ionic liquid, which allows it to remain stable for a longer period. This may be the reason why the gel sample without IL exhibited higher weight loss compared with the gel with IL exhibiting more stability at 200 and 350 °C [63,64]. A similar kind of behavior in the improvement of ionic liquid thermal stability was observed by Vekariya et al. [25]. Overall, gels prepared using IL exhibited higher thermal stability compared with the control gel.

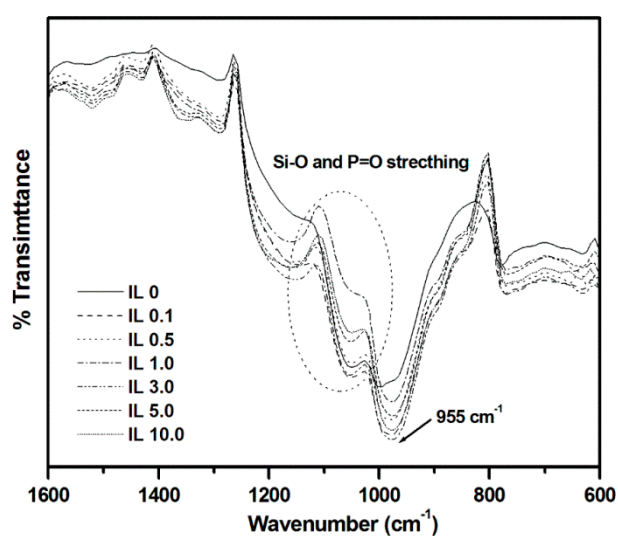


Figure 1. Expanded regions (600–1600  $\text{cm}^{-1}$ ) of FT-IR spectra for the wet silica ionogels.

Table 2. TGA data of wet silica ionogels.

Codes	TGA
	Weight Loss at 100 °C (%)
IL 0	13.1
IL 0.1	11.6
IL 0.5	10.9
IL 1.0	10.2
IL 3.0	9.4
IL 5.0	9.2
IL 10.0	8.5

### 3.3. $\text{N}_2$ Adsorption Isotherm

Figure 2 depicts the  $\text{N}_2$  adsorption–desorption isotherms of control silica gel (IL 0) and ionogel (IL 10). The isotherms are typical type IV, indicating a mesoporous nature according to IUPAC classification [65]. Control silica gel shows an H2 hysteresis loop of a type IV isotherm, whereas the ionogel shows an H3 hysteresis loop of type IV, representing mesoporous materials. The isotherm of the H3 loop with a sharp upturn in the high relative pressure range was observed for silica ionogels that underwent freeze-drying. This indicates that the pore network is comprised of macropores in the structure where the

liquid is not completely condensed [66]. The average pore size of the control gel was found to be 10.7 nm, whereas the pore size of the ionogel was 12.2 nm. It is clearly observed that on increasing the ionic liquid content in the gel, the average pore size increases. Such an obvious trend of pore size was reported for an ionogel prepared by loading ionic liquid in a porous silica gel matrix [67].

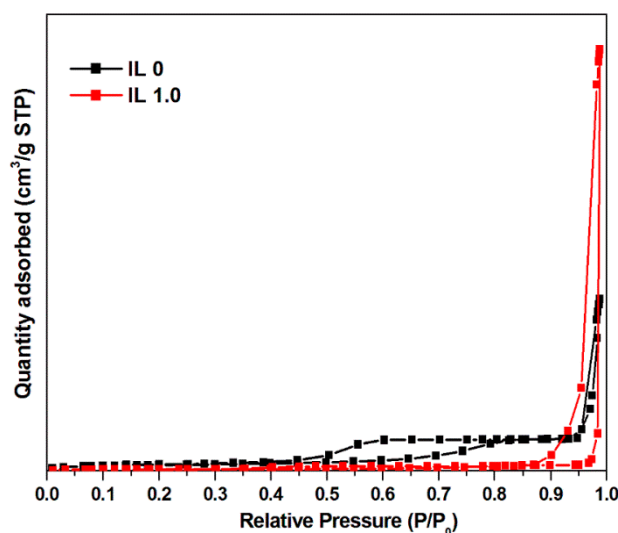


**Figure 2.** N<sub>2</sub> adsorption/desorption isotherm plot for the prepared gel samples.

### 3.4. Solid-State NMR Spectra

The formation of a silica network structure was confirmed using <sup>29</sup>Si solid-state NMR, and the spectra are provided in Figure S3. The <sup>29</sup>Si NMR spectrum of the control gel (IL 0) gives three major signals at −93, −103, and −111 ppm, corresponding to Q<sup>2</sup>, Q<sup>3</sup>, and Q<sup>4</sup> environments, respectively [68,69]. All the gel samples exhibited a prominent Q<sup>4</sup> peak at around −110 ppm. This shows the formation of completely condensed silica species. The introduction of ionic liquid favors the formation of a more interconnected network structure. On increasing the concentration of IL, the peak intensities of Q<sup>2</sup> and Q<sup>3</sup> environments decreased. In the case of IL 10.0, only one single broad peak was observed at −112 ppm. The appearance of the Q<sup>4</sup> peak confirms the formation of a completely condensed network structure. The increase in IL concentration accelerates the condensation of silanol groups present in silica ionogel surface [19]. This is evidence of the formation of a completely interconnected silica network structure. Overall, <sup>29</sup>Si solid-state CP/MAS NMR spectra provide clear information about the highly cross-linked and condensed states of siloxane linkages present in the gels.

### 3.5. Rheological Studies

The viscoelastic properties of the silica sols prepared using ionic liquid were studied by time-dependent rheological measurements at 25 °C. The time-dependent rheological curves are given in Figure 3. All the prepared gel samples exhibited a G' > G'' trend, which is the characteristic feature of a strongly viscoelastic gel system [70]. The gelation time was defined as the time required to reach a constant storage modulus G' of a viscoelastic material [71]. We noted the gelation time as the maximum time required to reach a constant modulus value. In the case of gel prepared without ionic liquid (IL 0), the sol took more time to become a gel and the gelation time was higher (t<sub>gel</sub> = 1800 s). The addition of ionic liquid enhances the cross-linking, thereby decreasing the gelation time, which can be seen from gelation time values for the gel prepared with IL. The decrease in gelation time was observed for imidazolium ionic liquid bearing organically modified silica (ORMOSIL) compared with pure silica [72]. Moreover, DNA ionogels containing IL (1-ethyl-3-methyl imidazolium chloride) show a decreasing trend in gelation time from 400 to 250 s for

1% and 5% IL concentrations, respectively [73]. Sannigrahi et al. [74] reported that the addition of a higher polymer concentration and lower gelation temperature allows faster gelation time and rate in the gelation kinetics of polybenzimidazole in phosphoric acid solution. The gelation time for the gel prepared with a higher IL (IL 10.0) content was 1100 s. The gel prepared with IL (10 wt %) showed a higher  $G'$  value than that of gel without ionic liquid. This can be attributed to the enhancement of cross-linking and ionic interaction between silica particles and IL. Further, we could observe a very steep rise in the complex viscosity ( $\eta^*$ ) of the silica sol system prepared using ionic liquid. Similar results were reported by Dawedeit et al. [75] for the sol solution of low-density aerogel. Overall, it is shown that silica ionogels with tunable gelation time can be prepared by varying different concentrations of ionic liquid. The gelation time is a measure of the elastic and viscous behavior of a viscoelastic material. The introduction of an ionic liquid promotes the formation of a more interconnected silica network structure. This clearly proves the strong interaction between silica particles and ionic liquid, which enhances network formation [76].

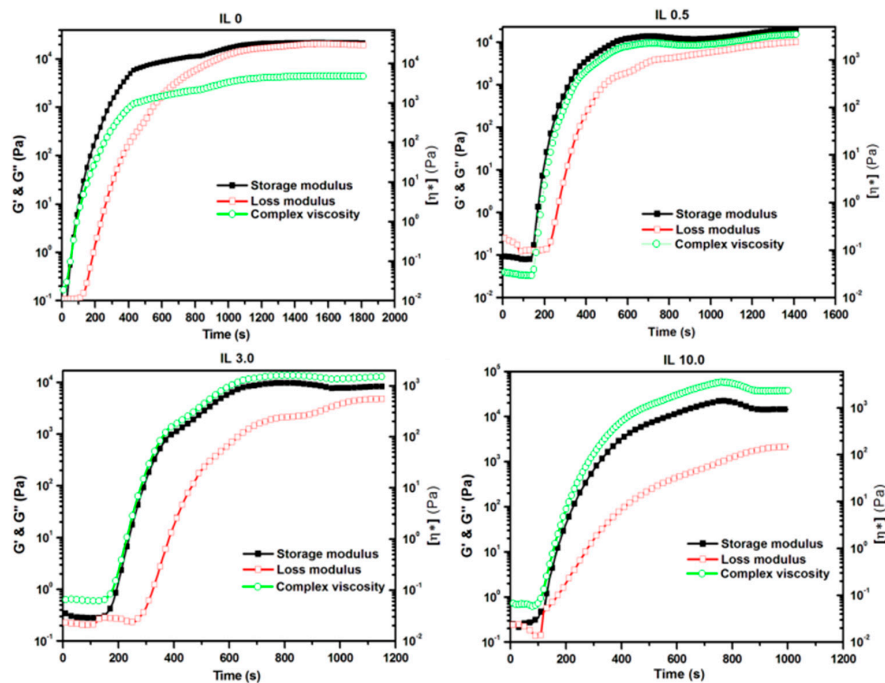


**Figure 3.** Time-dependent rheological studies of storage modulus ( $G'$ ), loss modulus ( $G''$ ), and complex viscosity ( $\eta^*$ ) for the silica sols prepared using ionic liquid.

### 3.6. Particle Size Analyses

The role of IL in the particle size of silica ionogel ground powder was studied using particle size measurement and their particle size distribution (PSD) plot, provided in Figure S4. The Z-average particle size (radius) of gel prepared without ionic liquid was found to be 470 nm. The particle size increased upon the addition of ionic liquid for 3 wt % of IL. The particle size of silica ionogel (IL 3.0) was 506 nm, with an increase in intensity of the peak. Further, addition of IL gives a bimodal size distribution, whereas the control gel shows only a monomodal size distribution. The PSD plot of IL 10.0 shows two peaks correspond to primary silica particles at 95 nm and agglomerated silica particles at 578 nm. The presence of a higher amount of IL may agglomerate the silica particles [52,53]. According to Dai et al. [18], the high ionic strength of ionic liquids increases the rate of particle aggregation when used as the solvent for the sol–gel process. This is clearly evident from the increased particle size with respect to ionic liquid content. However, the appearance



of bimodal size distribution for IL 10 resulted from the increased grinding time, since a high grinding time decreases the volume of bigger particles and creates agglomeration of smaller particles similar to primary particles [77]. The presence of larger-sized agglomerated particles clearly demonstrates the presence of ionic interaction between silica particles and IL [54,55], which is already seen from the increase in intensity of Si-O vibration from FT-IR spectra (Figure S1).

### 3.7. XRD Analyses

The X-ray diffraction patterns for the freeze-dried gels are depicted in Figure S5. XRD patterns provide information about the amorphous nature of the gel samples. All the gel samples exhibit an amorphous nature and no crystalline pattern was observed in the entire range. The X-ray diffraction of all the gel samples shows a broad peak at  $22^\circ$ , corresponding to the characteristic of an amorphous silica (Si-O ordered structure) backbone [78]. The introduction of ionic liquid does not alter the amorphous nature of the silica unit. Further, the increase of ionic liquid content broadens the intensity of the amorphous silica peak [79]. Ionic liquid favors the formation of a more interconnected silica network upon increasing the concentration of ionic liquid [80], which increases the peak intensity at  $2\theta = 22^\circ$ . This clearly shows that the addition of IL does not affect the backbone of the silica network and helps to enhance gel network formation.

### 3.8. SAXS Analyses

The structural information of the ionogels was investigated using SAXS measurements. Figures S6 and S7 represent SAXS patterns of silica ionogels with different ionic liquid concentrations. SAXS patterns of silica ionogels are in agreement with the mesoporous silica structure [81]. It can be seen from the SAXS patterns that a strong signal was observed at the low  $q$  region for all the gel samples irrespective of ionic liquid concentration. The observed signal is in accordance with  $q^{-4}$  behavior corresponding to amorphous behavior [82]. A similar kind of peak interference with a peak maximum at  $q = 0.8 \text{ nm}^{-1}$  was already reported by Smarsly et al. [83] for mesoporous silica materials. Moreover, the scattering intensities of SAXS of ionogel samples indicate that silica gel matrix formed a network structure. Further, the silica gel matrix consists of agglomerated silica nanoparticles [84]. The increase in scattering intensity of the peak in the lower  $q$  range is due to the formation of more silica networks with respect to ionic liquid content [85].

### 3.9. SEM Studies

The structural morphology of the prepared gels was investigated using scanning electron microscopy, and their images given in Figure 4. The morphology of the control gel sample (Figure 4a) shows a denser structure with small particles because of the large shrinkage that took place during the aging process [86], whereas gel prepared with a smaller amount of IL exhibits a slightly porous structure with larger particles (Figure 4b). In the case of a higher amount of IL (5 and 10 wt %), the surface shows a highly porous structure [11–13]. The addition of IL to the silica gel dramatically influences the surface of the ionogels (Figure 4c,d). The presence of a higher size of silica particles ranging from 50 to 100 nm with disk-shaped pores has been reported for silica aerogel prepared with different types of ILs [57].

### 3.10. TEM Studies

The porous structure and particle nature of the prepared gels were analyzed using TEM, and their images given in Figure 5. The control gel (IL 0) sample shows a linked network structure of smaller silica particles [87]. Moreover, the smaller spherical silica particles are less uniform in shape [88]. TEM images of all the gel samples show a dark region corresponding to the silica gel matrix and a bright spot representing the distinct pores present in the gel [89]. The structure of the silica is in an aggregated state when the concentration of the ionic liquid is increased. In the case of a higher IL content (IL 3.0), the

structure of the gel becomes more porous, which can be seen in Figure 5d (marked with a white-colored arrow). TEM images provide a clear picture of the porous structure and particle nature of the prepared silica gels.

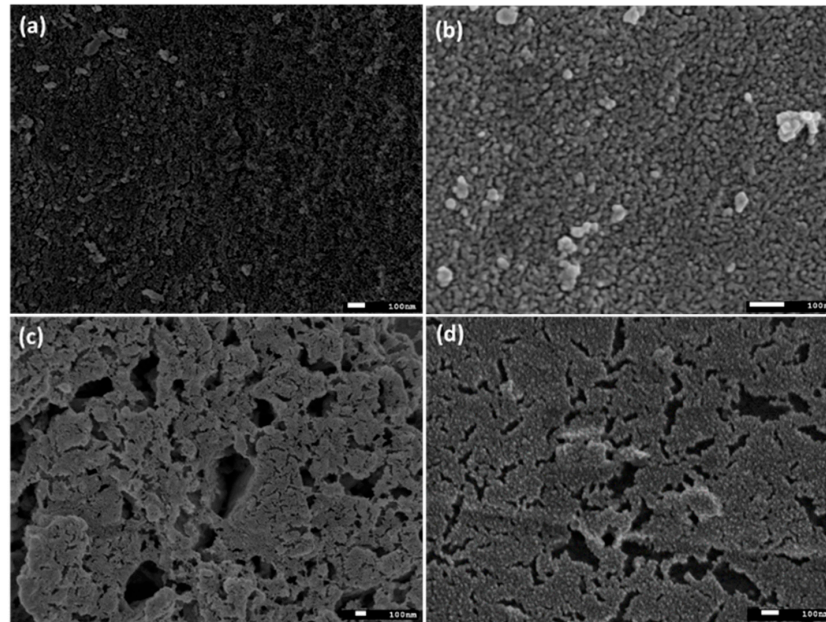


**Figure 4.** SEM images of silica ionogels: (a) IL 0 ( $\times 50$  K), (b) IL 1.0 ( $\times 100$  K), (c) IL 5.0 ( $\times 30$  K), and (d) IL 10.0 ( $\times 50$  K).

### 3.11. Biocompatibility Studies of the Ionogels

Cytocompatibility of the silica ionogel samples was studied using an MTT (3-(4,5-dimethylthiazol-2-yl)-2,5-diphenyl tetrazolium bromide) assay. Immortalized human epidermal keratinocytes HaCaT and Swiss fibroblast S3T6 cells were used for the assay. Twelve thousand cells per well were seeded in 48-well tissue culture plates and incubated for 24 h in a CO<sub>2</sub> incubator at 37 °C for the proliferation of cells. The seeded plates were treated with different concentrations (1, 5, 10, 25, 50, 75, and 100 µg/mL) of all the gel samples (IL 0, IL 0.1, IL 1.0, IL 3.0, IL 5.0, and IL 10.0). Then, after 24 h of incubation, MTT solution (0.5 mg/mL) was added and incubated for another 4 h at 37 °C. The formazan complex was solubilized with dimethyl sulfoxide, and adsorption was measured using a microplate reader at 570 nm.

The cytocompatibility of the ionogels with different concentrations of ionic liquids for Swiss fibroblast and HaCaT cells is presented in Figure 6. The % cell viability of IL 0 was found to be 76.75% and 99% for the lowest concentration of 1 µg/mL in Swiss fibroblast and HaCaT cells, respectively. In the case of the highest concentration of 100 µg/mL, the % cell viability was 17.43% and 20.3% in Swiss fibroblast and HaCaT cells, respectively. In the case of IL 0.1, 89.9% and 98% cell viability was observed for the lowest concentration of 1 µg/mL in Swiss fibroblast and HaCaT cells, respectively. In the case of a higher concentration (100 µg/mL), the % cell viability was estimated as 19.45% and 23.1% in Swiss fibroblast and HaCaT cells, respectively. The half-maximal inhibitory concentration (IC<sub>50</sub>) value was observed above 10 µg/mL for both cells. The gel sample IL 1.0 showed 85.6% and 95% cell viability for the minimum concentration of 1 µg/mL in Swiss fibroblast and HaCaT cells, respectively. The cell viability was reduced to 32.4% and 13.9% in Swiss fibroblast and HaCaT cells, respectively, for the higher concentration of the 100 µg/mL sample. The IL 3.0 sample exhibited 80.8% and 97% viability for both cells at the minimum concentration of 1 µg/mL, whereas the higher dose (100 µg/mL) showed 22.9% and 27% viability for both types of cells. The MTT assay indicates that 99.5% and 97% viability of cells was observed for IL 5.0 in both cells with a dose of 1 µg/mL. The higher dose of 100 µg/mL relatively

showed 20% and 16% in the tested cells. The IL 10 sample clearly exhibited 88.46% and 89% cell viability for the 1  $\mu\text{g}/\text{mL}$  dose concentration in Swiss fibroblast and HaCaT cells, respectively. The cell viability was observed as 20% and 21.5% in the 100  $\mu\text{g}/\text{mL}$  dose of the sample in both the cells. Overall, more than 50% cell viability (Swiss fibroblast and HaCaT cells) was observed for all the gel samples till the 10  $\mu\text{g}/\text{mL}$  concentration. The micrographs of the Swiss and HaCaT cell lines treated with various gel samples with a concentration 1  $\mu\text{g}/\text{mL}$  are provided in Figures 7 and 8. It can be observed from Figure 6 that gel samples provided very good viability and proliferation to HaCaT cell lines for the different concentrations of ionic-liquid-loaded ionogel samples (>90%). The addition of ionic liquid greatly influenced the Swiss cell viability of the IL 5.0 sample (99.5%) compared with the gel without ionic liquid (IL 0 (76%)). After 5% IL content, the Swiss cell viability decreased to 88%. The MTT assay clearly indicates that the prepared gel samples exhibit very good biocompatibility, which helps us to encapsulate biomolecules and retain their stability over a period.

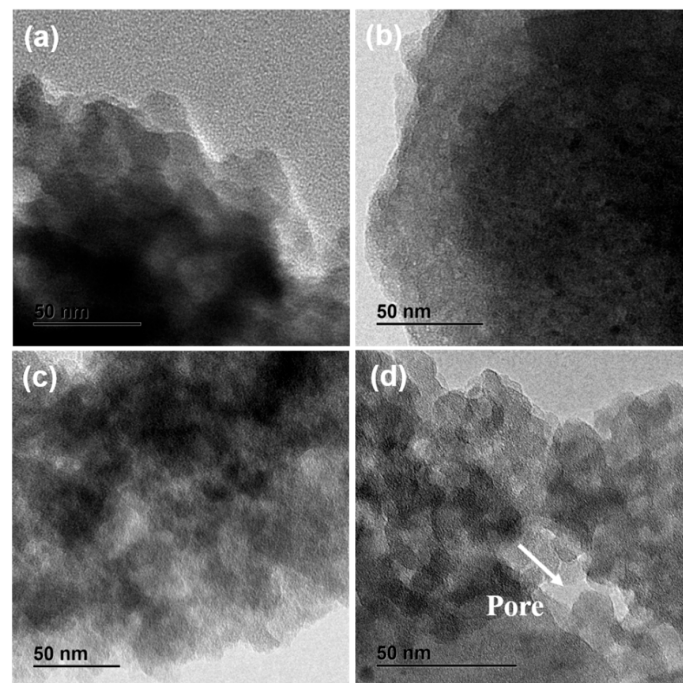


**Figure 5.** TEM images of the prepared silica ionogels: (a) IL 0, (b) IL 0.1, (c) IL 0.5, and (d) IL 3.0.

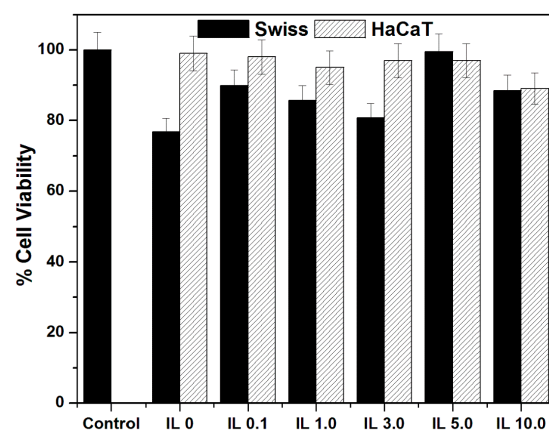


**Figure 6.** MTT assay of all the gel samples with 1  $\mu\text{g}/\text{mL}$  concentration on Swiss and HaCaT cells, respectively.

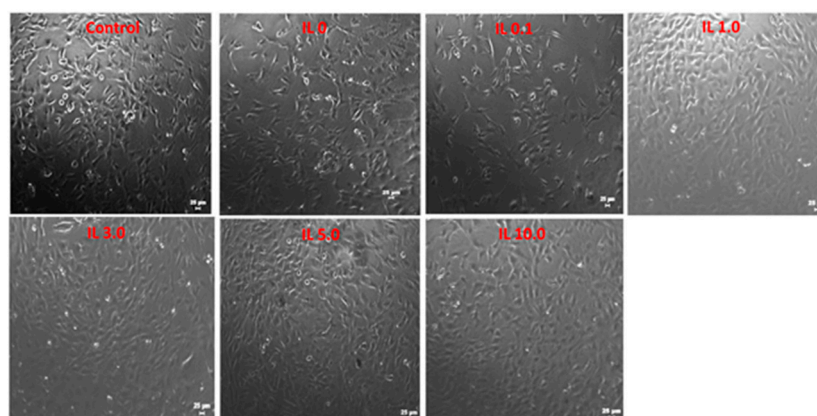


**Figure 7.** Morphological changes observed in the Swiss cells for the treatment with gels samples for a concentration of 1 µg/mL.

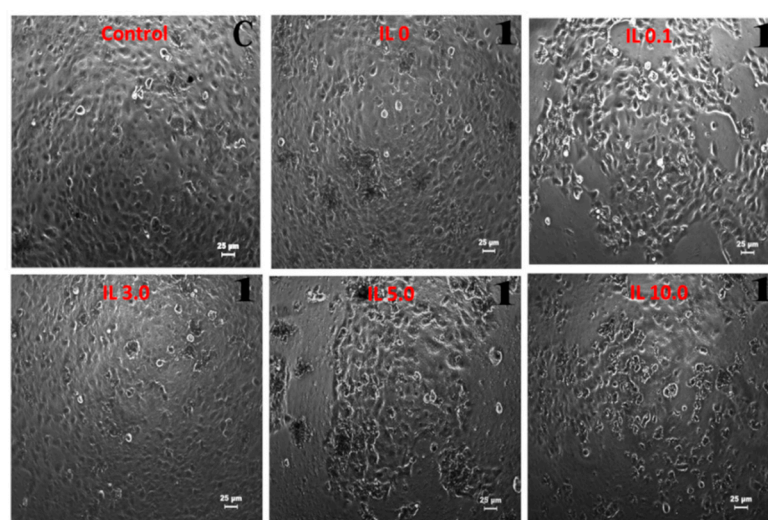


**Figure 8.** Morphological changes observed in the HaCaT cells for the treatment with gels samples for a concentration of 1 µg/mL.

#### 4. Conclusions

We have successfully synthesized silica-based ionogels using a biocompatible green solvent called choline dihydrogen phosphate ionic liquid at room temperature. The role of IL in the structural, thermal, viscoelastic, and morphological properties was investigated using various analytical techniques. FT-IR spectra confirmed the formation of a silica network structure and the presence of ionic liquid in the gel matrix. TGA studies showed that the confinement of IL improves the thermal stability of the prepared gels. Moreover, the formation of a siloxane network structure was evidenced from  $^{29}\text{Si}$  solid-state NMR spectra. The presence of ionic liquid improves the rheological properties of the silica sols. Rheological studies show that gels with tunable gelation times can be prepared by changing the amount of IL. XRD patterns clearly indicate the amorphous nature of the prepared gels. Furthermore, SEM and TEM images confirm the particle structure and porous nature of the gel samples prepared with ionic liquid. The MTT assay confirmed that all the gel samples exhibit 50% cell viability in Swiss and HaCaT cells for concentrations up to 5 µg/L. Hence, these ionogels could act as an excellent host material for biological molecules.

**Supplementary Materials:** The following are available online at <https://www.mdpi.com/2076-3417/11/1/206/s1>, Figure S1: FT-IR, Figure S2: TGA, Figure S3: Solid-state NMR, Figure S4: Particle size, Figure S5: XRD, and Figures S6 and S7: SAXS.

**Author Contributions:** Conceptualization, S.M.K.M., S.N.J., and A.B.M.; methodology, S.M.K.M. and R.M.S.; formal analysis, S.M.K.M., R.M.S., and M.S.K.; data curation, S.M.K.M.; writing—original draft preparation, S.M.K.M.; writing—review and editing, S.N.J., A.B.M., and B.M.; supervision, S.N.J. and A.B.M. All authors have read and agreed to the published version of the manuscript.

**Funding:** This research received no external funding.

**Institutional Review Board Statement:** Not applicable.

**Informed Consent Statement:** Not applicable.

**Data Availability Statement:** Data sharing not applicable.

**Acknowledgments:** One of the authors (S.M.K.M.) acknowledges CSIR, India (grant number 31/6(362)/2012-EMR-I) for the Senior Research Fellowship. A.B.M. is grateful to the Indian National Academy of Engineering (INAE) and CSIR-CGCRI for INAE Distinguished Professorship. We are grateful to V.G. Vaidyanathan and S.M. Jaimohan, CSIR-CLRI, for their support in SAXS analysis.

**Conflicts of Interest:** The authors declare no conflict of interest.

## References

- Schwan, M.; Ratke, L. Flexibilisation of resorcinol-formaldehyde aerogels. *J. Mater. Chem. A* **2013**, *1*, 13462–13468. [[CrossRef](#)]
- Ziegler, C.; Wolf, A.; Liu, W.; Herrmann, A.-K.; Gaponik, N.; Eychmüller, A. Modern Inorganic Aerogels. *Angew. Chem. Int. Ed.* **2017**, *56*, 13200–13221. [[CrossRef](#)] [[PubMed](#)]
- Zhao, S.; Siqueira, G.; Drdova, S.; Norris, D.; Ubert, C.; Bonnini, A.; Galmarini, S.; Ganobjak, M.; Pan, Z.; Brunner, S.; et al. Additive manufacturing of silica aerogels. *Nature* **2020**, *584*, 387–392. [[CrossRef](#)] [[PubMed](#)]
- Long, D.; Zhang, R.; Qiao, W.; Zhang, L.; Liang, X.; Ling, L. Biomolecular adsorption behavior on spherical carbon aerogels with various mesopore sizes. *J. Colloid Interface Sci.* **2009**, *331*, 40–46. [[CrossRef](#)]
- El-Safty, S.A.; Shahat, A.; Ismael, M. Mesoporous aluminosilica monoliths for the adsorptive removal of small organic pollutants. *J. Hazard. Mater.* **2012**, *201–202*, 23–32. [[CrossRef](#)]
- Lee, S.; Cha, Y.C.; Hwang, H.J.; Moon, J.-W.; Han, I.S. The effect of pH on the physicochemical properties of silica aerogels prepared by an ambient pressure drying method. *Mater. Lett.* **2007**, *61*, 3130–3133. [[CrossRef](#)]
- Bhatia, R.B.; Brinker, C.J.; Gupta, A.K.; Singh, A.K. Aqueous Sol-Gel Process for Protein Encapsulation. *Chem. Mater.* **2000**, *12*, 2434–2441. [[CrossRef](#)]
- Jin, W.; Brennan, J.D. Properties and applications of proteins encapsulated within sol-gel derived materials. *Analytica Chimica Acta* **2002**, *461*, 1–36. [[CrossRef](#)]
- Li, Y.K.; Chou, M.J.; Wu, T.-Y.; Jinn, T.-R.; Chen-Yang, Y.W. A novel method for preparing a protein-encapsulated bioaerogel: Using a red fluorescent protein as a model. *Acta Biomaterialia* **2008**, *4*, 725–732. [[CrossRef](#)]
- Nita, L.E.; Ghilan, A.; Rusu, A.G.; Neamtu, I.; Chiriac, A.P. New Trends in Bio-Based Aerogels. *Pharmaceutics* **2020**, *12*, 449. [[CrossRef](#)]
- Chen, S.; Zhang, S.; Liu, X.; Wang, J.; Wang, J.; Dong, K.; Sun, J.; Xu, B. Ionic liquid clusters: Structure, formation mechanism, and effect on the behavior of ionic liquids. *Phys. Chem. Chem. Phys.* **2014**, *16*, 5893–5906. [[CrossRef](#)] [[PubMed](#)]
- Wu, F.; Chen, N.; Chen, R.; Wang, L.; Li, L. Organically modified silica-supported ionogels electrolyte for high temperature lithium-ion batteries. *Nano Energy* **2017**, *31*, 9–18. [[CrossRef](#)]
- Tröger-Müller, S.; Brandt, J.; Antonietti, M.; Liedel, C. Green Imidazolium Ionics—From Truly Sustainable Reagents to Highly Functional Ionic Liquids. *Chem. Eur. J.* **2017**, *23*, 11810–11817. [[CrossRef](#)]
- Donato, R.K.; Matějka, L.; Schrekker, H.S.; Pleštil, J.; Jigounov, A.; Brus, J.; Šlouf, M. The multifunctional role of ionic liquids in the formation of epoxy-silica nanocomposites. *J. Mater. Chem.* **2011**, *21*, 13801–13810. [[CrossRef](#)]
- Sun, J.-K.; Antonietti, M.; Yuan, J. Nanoporous ionic organic networks: From synthesis to materials applications. *Chem. Soc. Rev.* **2016**, *45*, 6627–6656. [[CrossRef](#)] [[PubMed](#)]
- Martinelli, A.; Nordstierna, L. An investigation of the sol-gel process in ionic liquid-silica gels by time resolved Raman and <sup>1</sup>H NMR spectroscopy. *Phys. Chem. Chem. Phys.* **2012**, *14*, 13216–13223. [[CrossRef](#)] [[PubMed](#)]
- Viau, L.; Néouze, M.-A.; Biolley, C.; Volland, S.; Brevet, D.; Gaveau, P.; Dieudonné, P.; Galarneau, A.; Vioux, A. Ionic Liquid Mediated Sol-Gel Synthesis in the Presence of Water or Formic Acid: Which Synthesis for Which Material? *Chem. Mater.* **2012**, *24*, 3128–3134. [[CrossRef](#)]
- Dai, S.; Ju, Y.H.; Gao, H.J.; Lin, J.S.; Pennycook, S.J.; Barnes, C.E. Preparation of silica aerogel using ionic liquids as solvents. *Chem. Commun.* **2000**, 243–244. [[CrossRef](#)]
- Migliorini, M.V.; Donato, R.K.; Benvegnú, M.A.; Gonçalves, R.S.; Schrekker, H.S. Imidazolium ionic liquids as bifunctional materials (morphology controller and pre-catalyst) for the preparation of xerogel silica's. *J. Sol Gel Sci. Technol.* **2008**, *48*, 272–276. [[CrossRef](#)]
- Vioux, A.; Viau, L.; Volland, S.; Le Bideau, J. Use of ionic liquids in sol-gel; ionogels and applications. *Comptes Rendus Chimie* **2010**, *13*, 242–255. [[CrossRef](#)]

21. Le Bideau, J.; Viau, L.; Vioux, A. Ionogels, ionic liquid based hybrid materials. *Chem. Soc. Rev.* **2011**, *40*, 907–925. [[CrossRef](#)] [[PubMed](#)]
22. Lunstroot, K.; Driesen, K.; Nockemann, P.; Van Hecke, K.; Van Meervelt, L.; Görlner-Walrand, C.; Binnemans, K.; Bellayer, S.; Viau, L.; Le Bideau, J.; et al. Lanthanide-Doped luminescent ionogels. *Dalton Trans.* **2009**, 298–306. [[CrossRef](#)] [[PubMed](#)]
23. Néouze, M.-A.; Le Bideau, J.; Gaveau, P.; Bellayer, S.; Vioux, A. Ionogels, New Materials Arising from the Confinement of Ionic Liquids within Silica-Derived Networks. *Chem. Mater.* **2006**, *18*, 3931–3936. [[CrossRef](#)]
24. Gupta, A.K.; Singh, R.K.; Chandra, S. Studies on mesoporous silica ionogels prepared by sol-gel method at different gelation temperatures. *RSC Adv.* **2013**, *3*, 13869–13877. [[CrossRef](#)]
25. Vekariya, R.L.; Dhar, A.; Lunagariya, J. Synthesis and characterization of double-SO<sub>3</sub>H functionalized Brønsted acidic hydrogen-sulfate ionic liquid confined with silica through sol-gel method. *Compos. Interfaces* **2017**, *24*, 801–816. [[CrossRef](#)]
26. Xue, C.; Zhu, H.; Du, X.; An, X.; Wang, E.; Duan, D.; Shi, L.; Hao, X.; Xiao, B.; Peng, C. Unique allosteric effect-driven rapid adsorption of carbon dioxide in a newly designed ionogel [P4444][2-Op]@MCM-41 with excellent cyclic stability and loading-dependent capacity. *J. Mater. Chem. A* **2017**, *5*, 6504–6514. [[CrossRef](#)]
27. Göbel, R.; Friedrich, A.; Taubert, A. Tuning the phase behavior of ionic liquids in organically functionalized silica ionogels. *Dalton Trans.* **2010**, 39, 603–611. [[CrossRef](#)]
28. Göbel, R.; White, R.J.; Titirici, M.-M.; Taubert, A. Carbon-Based ionogels: Tuning the properties of the ionic liquid via carbon-ionic liquid interaction. *Phys. Chem. Chem. Phys.* **2012**, *14*, 5992–5997. [[CrossRef](#)]
29. Sharma, M.; Mondal, D.; Mukesh, C.; Prasad, K. Preparation of tamarind gum based soft ion gels having thixotropic properties. *Carbohydr. Polym.* **2014**, *102*, 467–471. [[CrossRef](#)]
30. Viau, L.; Tourné-Péteilh, C.; Devoisselle, J.-M.; Vioux, A. Ionogels as drug delivery system: One-step sol-gel synthesis using imidazolium ibuprofenate ionic liquid. *Chem. Commun.* **2010**, 46, 228–230. [[CrossRef](#)]
31. Sen, K.; Mendes, E.; Wolterbeek, H.T. Combined effort of Fe-dextran and an RTIL towards formation of ionogel. *J. Sol Gel Sci. Technol.* **2012**, *63*, 135–139. [[CrossRef](#)]
32. Trivedi, T.J.; Rao, K.S.; Kumar, A. Facile preparation of agarose-chitosan hybrid materials and nanocomposite ionogels using an ionic liquid via dissolution, regeneration and sol-gel transition. *Green Chem.* **2014**, *16*, 320–330. [[CrossRef](#)]
33. Subianto, S.; Mistry, M.K.; Choudhury, N.R.; Dutta, N.K.; Knott, R. Composite Polymer Electrolyte Containing Ionic Liquid and Functionalized Polyhedral Oligomeric Silsesquioxanes for Anhydrous PEM Applications. *ACS Appl. Mater. Interfaces* **2009**, *1*, 1173–1182. [[CrossRef](#)] [[PubMed](#)]
34. Chu, F.; Lin, B.; Yan, F.; Qiu, L.; Lu, J. Macromolecular protic ionic liquid-based proton-conducting membranes for anhydrous proton exchange membrane application. *J. Power Sources* **2011**, *196*, 7979–7984. [[CrossRef](#)]
35. Maity, S.; Singha, S.; Jana, T. Low acid leaching PEM for fuel cell based on polybenzimidazole nanocomposites with protic ionic liquid modified silica. *Polymer* **2015**, *66*, 76–85. [[CrossRef](#)]
36. Aquino, S.A.; Vieira, M.O.; Ferreira, A.S.D.; Cabrita, E.J.; Einloft, S.; de Souza, M.O. Hybrid Ionic Liquid-Silica Xerogels Applied in CO<sub>2</sub> Capture. *Appl. Sci.* **2019**, *9*, 2614. [[CrossRef](#)]
37. Lee, S.H.; Doan, T.T.N.; Ha, S.H.; Koo, Y.-M. Using ionic liquids to stabilize lipase within sol-gel derived silica. *J. Mol. Catal. B Enzym.* **2007**, *45*, 57–61. [[CrossRef](#)]
38. Liu, Y.; Wang, M.; Li, J.; Li, Z.; He, P.; Liu, H.; Li, J. Highly active horseradish peroxidase immobilized in 1-butyl-3-methylimidazolium tetrafluoroborate room-temperature ionic liquid based sol-gel host materials. *Chem. Commun.* **2005**, 1778–1780. [[CrossRef](#)]
39. Wood, N.; Stephens, G. Accelerating the discovery of biocompatible ionic liquids. *Phys. Chem. Chem. Phys.* **2010**, *12*, 1670–1674. [[CrossRef](#)]
40. Li, Z.; Liu, X.; Pei, Y.; Wang, J.; He, M. Design of environmentally friendly ionic liquid aqueous two-phase systems for the efficient and high activity extraction of proteins. *Green Chem.* **2012**, *14*, 2941–2950. [[CrossRef](#)]
41. Winther-Jensen, O.; Vijayaraghavan, R.; Sun, J.; Winther-Jensen, B.; MacFarlane, D.R. Self polymerising ionic liquid gel. *Chem. Commun.* **2009**, 3041–3043. [[CrossRef](#)] [[PubMed](#)]
42. Schröder, C. Proteins in Ionic Liquids: Current Status of Experiments and Simulations. *Top. Curr. Chem.* **2017**, *375*, 127–152. [[CrossRef](#)]
43. Elhi, F.; Priks, H.; Rinne, P.; Kaldalu, N.; Žusinaite, E.; Johanson, U.; Aabloo, A.; Tamm, T.; Pöhako-Esko, K. Electromechanically active polymer actuators based on biofriendly choline ionic liquids. *Smart Mater. Struct.* **2020**, *29*, 055021. [[CrossRef](#)]
44. Silva, L.P.; Moya, C.; Sousa, M.; Santiago, R.; Sintra, T.E.; Carreira, A.R.F.; Palomar, J.; Coutinho, J.A.P.; Carvalho, P.J. Encapsulated Amino-Acid-Based Ionic Liquids for CO<sub>2</sub> Capture. *Eur. J. Inorg. Chem.* **2020**, 2020, 3158–3166. [[CrossRef](#)]
45. Foureau, D.M.; Vrikkis, R.M.; Jones, C.P.; Weaver, K.D.; MacFarlane, D.R.; Salo, J.C.; McKillop, I.H.; Elliott, G.D. In Vitro Assessment of Choline Dihydrogen Phosphate (CDHP) as a Vehicle for Recombinant Human Interleukin-2 (rhIL-2). *Cell. Mol. Bioeng.* **2012**, *5*, 390–401. [[CrossRef](#)]
46. Fujita, K.; MacFarlane, D.R.; Forsyth, M. Protein solubilising and stabilising ionic liquids. *Chem. Commun.* **2005**, 4804–4806. [[CrossRef](#)]
47. Weaver, K.D.; Vrikkis, R.M.; Van Vorst, M.P.; Trullinger, J.; Vijayaraghavan, R.; Foureau, D.M.; McKillop, I.H.; MacFarlane, D.R.; Krueger, J.K.; Elliott, G.D. Structure and function of proteins in hydrated choline dihydrogen phosphate ionic liquid. *Phys. Chem. Chem. Phys.* **2012**, *14*, 790–801. [[CrossRef](#)]

48. Fujita, K.; MacFarlane, D.R.; Forsyth, M.; Yoshizawa-Fujita, M.; Murata, K.; Nakamura, N.; Ohno, H. Solubility and Stability of Cytochrome c in Hydrated Ionic Liquids: Effect of Oxo Acid Residues and Kosmotropicity. *Biomacromolecules* **2007**, *8*, 2080–2086. [[CrossRef](#)]
49. Mukesh, C.; Mondal, D.; Sharma, M.; Prasad, K. Rapid dissolution of DNA in a novel bio-based ionic liquid with long-term structural and chemical stability: Successful recycling of the ionic liquid for reuse in the process. *Chem. Commun.* **2013**, *49*, 6849–6851. [[CrossRef](#)]
50. Hoshino, T.; Fujita, K.; Higashi, A.; Sakiyama, K.; Ohno, H.; Morishima, K. Contracting cardiomyocytes in hydrophobic room-temperature ionic liquid. *Biochem. Biophys. Res. Commun.* **2012**, *427*, 379–384. [[CrossRef](#)]
51. Tateishi-Karimata, H.; Sugimoto, N. A-T Base Pairs are More Stable than G-C Base Pairs in a Hydrated Ionic Liquid. *Angewandte Chemie* **2012**, *51*, 1416–1419. [[CrossRef](#)] [[PubMed](#)]
52. Meera, K.M.S.; Sankar, R.M.; Jaisankar, S.N.; Mandal, A.B. Mesoporous and biocompatible surface active silica aerogel synthesis using choline formate ionic liquid. *Colloids Surf. B Biointerfaces* **2011**, *86*, 292–297. [[CrossRef](#)] [[PubMed](#)]
53. Seeni Meera, K.; Murali Sankar, R.; Jaisankar, S.N.; Baran Mandal, A. Studies on Biocompatible Surface-Active Silica Aerogel and Polyurethane-Siloxane Cross-Linked Structures for Various Surfaces. In *Encyclopedia of Biocolloid and Biointerface Science 2V Set*; Ohshima, H., Ed.; Wiley: Hoboken, NJ, USA, 2016; pp. 1–16.
54. Seeni Meera, K.M.; Murali Sankar, R.; Murali, A.; Jaisankar, S.N.; Mandal, A.B. Sol-Gel network silica/modified montmorillonite clay hybrid nanocomposites for hydrophobic surface coatings. *Colloids Surf. B Biointerfaces* **2012**, *90*, 204–210. [[CrossRef](#)] [[PubMed](#)]
55. Delahaye, E.; Göbel, R.; Löbbicke, R.; Guillot, R.; Sieber, C.; Taubert, A. Silica ionogels for proton transport. *J. Mater. Chem.* **2012**, *22*, 17140–17146. [[CrossRef](#)]
56. Silverstein, R.M.; Webster, F.X.; Kiemle, D.J. *Spectrometric Identification of Organic Compounds*; John Wiley and Sons: Hoboken, NJ, USA, 2005.
57. Karout, A.; Pierre, A.C. Porous texture of silica aerogels made with ionic liquids as gelation catalysts. *J. Sol Gel Sci. Technol.* **2009**, *49*, 364–372. [[CrossRef](#)]
58. Ashby, D.S.; DeBlock, R.H.; Lai, C.-H.; Choi, C.S.; Dunn, B.S. Patternable, Solution-Processed Ionogels for Thin-Film Lithium-Ion Electrolytes. *Joule* **2017**, *1*, 344–358. [[CrossRef](#)]
59. Verma, Y.L.; Gupta, A.K.; Singh, R.K.; Chandra, S. Preparation and characterisation of ionic liquid confined hybrid porous silica derived from ultrasonic assisted non-hydrolytic sol-gel process. *Microporous Mesoporous Mater.* **2014**, *195*, 143–153. [[CrossRef](#)]
60. Yoshizawa-Fujita, M.; Fujita, K.; Forsyth, M.; MacFarlane, D.R. A new class of proton-conducting ionic plastic crystals based on organic cations and dihydrogen phosphate. *Electrochem. Commun.* **2007**, *9*, 1202–1205. [[CrossRef](#)]
61. Rana, U.A.; Bayley, P.M.; Vijayaraghavan, R.; Howlett, P.; MacFarlane, D.R.; Forsyth, M. Proton transport in choline dihydrogen phosphate/H<sub>3</sub>PO<sub>4</sub> mixtures. *Phys. Chem. Chem. Phys.* **2010**, *12*, 11291–11298. [[CrossRef](#)]
62. Wang, X.; Jana, S.C. Synergistic Hybrid Organic-Inorganic Aerogels. *ACS Appl. Mater. Interfaces* **2013**, *5*, 6423–6429. [[CrossRef](#)]
63. Bothwell, K.M.; Marr, P.C. Taming the Base Catalyzed Sol-Gel Reaction: Basic Ionic Liquid Gels of SiO<sub>2</sub> and TiO<sub>2</sub>. *ACS Sustain. Chem. Eng.* **2017**, *5*, 1260–1263. [[CrossRef](#)]
64. Singh, M.P.; Singh, R.K.; Chandra, S. Ionic liquids confined in porous matrices: Physicochemical properties and applications. *Progress Mater. Sci.* **2014**, *64*, 73–120. [[CrossRef](#)]
65. Thommes, M.; Kaneko, K.; Neimark, A.V.; Olivier, J.P.; Rodriguez-Reinoso, F.; Rouquerol, J.; Sing, K.S.W. Physisorption of gases, with special reference to the evaluation of surface area and pore size distribution (IUPAC Technical Report). *J. Pure Appl. Chem.* **2015**, *87*, 1051–1069. [[CrossRef](#)]
66. Sert Çok, S.; Koç, F.; Balkan, F.; Gizli, N. Revealing the pore characteristics and physicochemical properties of silica ionogels based on different sol-gel drying strategies. *J. Solid State Chem.* **2019**, *278*, 120877. [[CrossRef](#)]
67. Gupta, A.K.; Singh, M.P.; Singh, R.K.; Chandra, S. Low density ionogels obtained by rapid gellification of tetraethyl orthosilane assisted by ionic liquids. *Dalton Trans.* **2012**, *41*, 6263–6271. [[CrossRef](#)]
68. Seeni Meera, K.M.; Murali Sankar, R.; Jaisankar, S.N.; Mandal, A.B. Physicochemical Studies on Polyurethane/Siloxane Cross-Linked Films for Hydrophobic Surfaces by the Sol-Gel Process. *J. Phys. Chem. B* **2013**, *117*, 2682–2694. [[CrossRef](#)]
69. Seeni Meera, K.M.; Murali Sankar, R.; Paul, J.; Jaisankar, S.N.; Mandal, A.B. The influence of applied silica nanoparticles on a bio-renewable castor oil based polyurethane nanocomposite and its physicochemical properties. *Phys. Chem. Chem. Phys.* **2014**, *16*, 9276–9288. [[CrossRef](#)]
70. Wang, G.-H.; Zhang, L.-M. A Biofriendly Silica Gel for in Situ Protein Entrapment: Biopolymer-Assisted Formation and Its Kinetic Mechanism. *J. Phys. Chem. B* **2009**, *113*, 2688–2694. [[CrossRef](#)]
71. Poolman, J.M.; Boekhoven, J.; Besselink, A.; Olive, A.G.L.; van Esch, J.H.; Eelkema, R. Variable gelation time and stiffness of low-molecular-weight hydrogels through catalytic control over self-assembly. *Nat. Protoc.* **2014**, *9*, 977–988. [[CrossRef](#)]
72. Carvalho, A.P.A.; Soares, B.G.; Livi, S. Organically modified silica (ORMOSIL) bearing imidazolium—Based ionic liquid prepared by hydrolysis/co-condensation of silane precursors: Synthesis, characterization and use in epoxy networks. *Eur. Polym. J.* **2016**, *83*, 311–322. [[CrossRef](#)]
73. Pandey, P.K.; Rawat, K.; Aswal, V.K.; Kohlbrecher, J.; Bohidar, H.B. DNA ionogel: Structure and self-assembly. *Phys. Chem. Chem. Phys.* **2017**, *19*, 804–812. [[CrossRef](#)] [[PubMed](#)]
74. Sannigrahi, A.; Ghosh, S.; Maity, S.; Jana, T. Polybenzimidazole gel membrane for the use in fuel cell. *Polymer* **2011**, *52*, 4319–4330. [[CrossRef](#)]

75. Dawedeit, C.; Kim, S.H.; Braun, T.; Worsley, M.A.; Letts, S.A.; Wu, K.J.; Walton, C.C.; Chernov, A.A.; Satcher, J.H.; Hamza, A.V.; et al. Tuning the rheological properties of sols for low-density aerogel coating applications. *Soft Matter* **2012**, *8*, 3518–3521. [[CrossRef](#)]
76. Song, H.; Luo, Z.; Zhao, H.; Luo, S.; Wu, X.; Gao, J.; Wang, Z. High tensile strength and high ionic conductivity bionanocomposite ionogels prepared by gelation of cellulose/ionic liquid solutions with nano-silica. *RSC Adv.* **2013**, *3*, 11665–11675. [[CrossRef](#)]
77. Rennie, A.J.R.; Martins, V.L.; Smith, R.M.; Hall, P.J. Influence of Particle Size Distribution on the Performance of Ionic Liquid-based Electrochemical Double Layer Capacitors. *Sci. Rep.* **2016**, *6*, 22062. [[CrossRef](#)] [[PubMed](#)]
78. Li, Q.-P.; Yan, B. Luminescent nanoparticles prepared by encapsulating lanthanide chelates to silica sphere. *Colloid Polym. Sci.* **2014**, *292*, 1385–1393. [[CrossRef](#)]
79. Ward, A.J.; Pujari, A.A.; Costanzo, L.; Masters, A.F.; Maschmeyer, T. Ionic liquid-templated preparation of mesoporous silica embedded with nanocrystalline sulfated zirconia. *Nanoscale Res. Lett.* **2011**, *6*, 192. [[CrossRef](#)]
80. Ak, F.; Oztoprak, Z.; Karakutuk, I.; Okay, O. Macroporous Silk Fibroin Cryogels. *Biomacromolecules* **2013**, *14*, 719–727. [[CrossRef](#)]
81. Polarz, S.; Smarsly, B. Nanoporous Materials. *J. Nanosci. Nanotechnol.* **2002**, *2*, 581–612. [[CrossRef](#)]
82. Taubert, A.; Löbbicke, R.; Kirchner, B.; Leroux, F. First examples of organosilica-based ionogels: Synthesis and electrochemical behavior. *Beilstein J. Nanotechnol.* **2017**, *8*, 736–751. [[CrossRef](#)]
83. Smarsly, B.; Göltner, C.; Antonietti, M.; Ruland, W.; Hoinkis, E. SANS Investigation of Nitrogen Sorption in Porous Silica. *J. Phys. Chem. B* **2001**, *105*, 831–840. [[CrossRef](#)]
84. Wu, C.-M.; Lin, S.-Y. Close Packing Existence of Short-Chain Ionic Liquid Confined in the Nanopore of Silica Ionogel. *J. Phys. Chem. C* **2015**, *119*, 12335–12344. [[CrossRef](#)]
85. Nayeri, M.; Nygård, K.; Karlsson, M.; Maréchal, M.; Burghammer, M.; Reynolds, M.; Martinelli, A. The role of the ionic liquid C6C1ImTFSI in the sol-gel synthesis of silica studied using in situ SAXS and Raman spectroscopy. *Phys. Chem. Chem. Phys.* **2015**, *17*, 9841–9848. [[CrossRef](#)] [[PubMed](#)]
86. Bhagat, S.D.; Kim, Y.-H.; Suh, K.-H.; Ahn, Y.-S.; Yeo, J.-G.; Han, J.-H. Superhydrophobic silica aerogel powders with simultaneous surface modification, solvent exchange and sodium ion removal from hydrogels. *Microporous Mesoporous Mater.* **2008**, *112*, 504–509. [[CrossRef](#)]
87. Aravind, P.R.; Shajesh, P.; Mukundan, P.; Warriar, K.G.K. Silica-Titania aerogel monoliths with large pore volume and surface area by ambient pressure drying. *J. Sol Gel Sci. Technol.* **2009**, *52*, 328–334. [[CrossRef](#)]
88. Göbel, R.; Hesemann, P.; Weber, J.; Möller, E.; Friedrich, A.; Beuermann, S.; Taubert, A. Surprisingly high, bulk liquid-like mobility of silica-confined ionic liquids. *Phys. Chem. Chem. Phys.* **2009**, *11*, 3653–3662. [[CrossRef](#)]
89. Wu, C.-M.; Lin, S.-Y.; Chen, H.-L. Structure of a monolithic silica aerogel prepared from a short-chain ionic liquid. *Microporous Mesoporous Mater.* **2012**, *156*, 189–195. [[CrossRef](#)]